

2001

Application of Dynamic System Identification to Timber Beams - part II

S T. Peterson
Washington State University

D I. McLean
Washington State University


M D. Symans
Washington State University

David Pollock
George Fox University, dpollock@georgefox.edu

W F. Cofer
Washington State University

See next page for additional authors

Follow this and additional works at: https://digitalcommons.georgefox.edu/mece_fac

 Part of the [Civil Engineering Commons](#), [Mechanical Engineering Commons](#), and the [Structural Materials Commons](#)

Recommended Citation

Peterson, S T.; McLean, D I.; Symans, M D.; Pollock, David; Cofer, W F.; Emerson, R N.; and Fridley, Kenneth J., "Application of Dynamic System Identification to Timber Beams - part II" (2001). *Faculty Publications - Biomedical, Mechanical, and Civil Engineering*. 34.
https://digitalcommons.georgefox.edu/mece_fac/34

This Article is brought to you for free and open access by the Department of Biomedical, Mechanical, and Civil Engineering at Digital Commons @ George Fox University. It has been accepted for inclusion in Faculty Publications - Biomedical, Mechanical, and Civil Engineering by an authorized administrator of Digital Commons @ George Fox University. For more information, please contact arolfe@georgefox.edu.

Authors

S T. Peterson, D I. McLean, M D. Symans, David Pollock, W F. Cofer, R N. Emerson, and Kenneth J. Fridley

APPLICATION OF DYNAMIC SYSTEM IDENTIFICATION TO TIMBER BEAMS. II

By S. T. Peterson,¹ D. I. McLean,² M. D. Symans,³ D. G. Pollock,⁴ W. F. Cofer,⁵
R. N. Emerson,⁶ and K. J. Fridley⁷

ABSTRACT: In a companion paper, a method of global nondestructive evaluation (NDE) for identifying local damage and decay in timber beams was developed and verified analytically using a finite-element model of a timber beam. The previously presented method of damage localization employs experimental modal analysis and an algorithm that monitors changes in modal strain energy between the mode shapes of a damaged beam with respect to the undamaged state of the beam. In this second part of a two-part paper, experimental laboratory tests on simply supported timber beams are presented to verify the capabilities and determine the limitations of the proposed method of NDE in locating simulated damage in simply supported timber beams. Due to the natural variability inherent within a timber beam, the required severity of inflicted damage before the algorithm could correctly identify damage location was a 5.08-cm (2-in.) deep saw cut in a beam with a depth of 15.88 cm (6.25 in.). For practical applications, the proposed technique could be used to identify the presence and general location of severe decay or damage, and if needed, more refined NDE techniques could be used to map the specific region affected by the decay or damage.

INTRODUCTION

Nondestructive evaluation (NDE) of wood is the science and art of determining the material properties and/or structural capacity of individual members or for an entire timber structure without impairing the member or structure in its usefulness for its intended purpose. A number of methods have been previously developed and implemented in the field of NDE for wood, including visual inspection, stress wave, drill resistance, radiography, ultrasonics, and deflection/vibration analysis (Emerson et al. 1998). Many of these methods are performed on a very localized scale and the evaluation of an entire structure using these methods can be very time-consuming and inefficient. Thus, it is desirable to develop a method of nondestructive testing for timber structures that can identify damage or decay from a global perspective. The method selected is deflection/vibration analysis, specifically, experimental modal analysis.

In conjunction with the experimental modal analysis, a method for identifying and locating the damage within a structure is needed. In this study, a method of damage localization was used that was based on previous studies of steel plate girders and highway bridges to localize and estimate the severity of damage within the structure using a limited number of modal parameters (Bolton et al. 1998; Stubbs et al. 1998). Several analytical studies have been published that verify the

performance of this damage localization and severity estimation algorithm (Garcia and Stubbs 1996; Stubbs et al. 1997).

In a companion paper (Peterson et al. 2001), analytical evaluations were performed on a simply supported timber beam plane-stress model. This was done to investigate the capabilities and limitations of the damage localization algorithm in locating simulated damage in a simplified timber beam configuration. In this paper, the method of damage localization is applied to experimental laboratory tests. Based on the results of the analytical evaluations and experimental testing, the effectiveness of using a global nondestructive evaluation method for identifying damage in timber beams is demonstrated.

EXPERIMENTAL LABORATORY TESTING OF SIMPLY SUPPORTED TIMBER BEAM

In the laboratory, a simply supported Douglas fir beam was tested to validate the use of the damage localization algorithm in detecting simulated damage in an actual timber beam. The beam cross section measured approximately 11.43 cm \times 15.88 cm (4.5 in. \times 6.25 in.), and the span was 4.83 m (15 ft 10 in.). The beam was impacted at the 1/4-point near the roller support using an instrumented impact hammer and the acceleration was measured at each of the 1/8-points along the span using accelerometers attached to the bottom (tension) face of the beam. No acceleration measurements were made at the supports, though this is typically recommended to better assess the actual support conditions. A concrete weight of approximately 22.7 kg (50 lb) was placed on the beam at midspan during the impact vibration tests to prevent the beam from bouncing on the supports. The impact force and acceleration response data were recorded at a sampling frequency of 1,000 Hz with 1,024 points of data collected per channel using a high-speed data acquisition system. For the undamaged case and each damaged case, 10 individual tests were performed and the normalized mode shape vectors from each test were averaged to remove some of the noise inherent in the data. Fig. 1 shows the experimental modal testing of the simply supported timber beam.

The beam was tested in its undamaged condition to establish the undamaged or baseline modal parameters. The beam was then progressively damaged by cutting notches out of the tension face of the beam located at the 1/4-point near the pin support. Magnitude of the inflicted damage for each damage case is given in Fig. 2. Inflicted damage in each case was centered at the 1/4-point, extending into the tension face of the beam. Damage case 5 is a stepped notch consisting of

¹Grad. Student, Dept. of Civ. and Envir. Engrg., Washington State Univ., Pullman, WA 99164-2910.

²Prof., Dept. of Civ. and Envir. Engrg., Washington State Univ., Pullman, WA 99164-2910.

³Asst. Prof., Dept. of Civ. and Envir. Engrg., Washington State Univ., Pullman, WA 99164-2910.

⁴Asst. Prof., Dept. of Civ. and Envir. Engrg., Washington State Univ., Pullman, WA 99164-2910.

⁵Assoc. Prof., Dept. of Civ. and Envir. Engrg., Washington State Univ., Pullman, WA 99164-2910.

⁶Asst. Prof., School of Civ. and Envir. Engrg., Oklahoma State Univ., Stillwater, OK 74078-5033.

⁷Prof., Dept. of Civ. and Envir. Engrg., Washington State Univ., Pullman, WA 99164-2910.

damage case 4 with an additional 2.54-cm deep \times 5.08-cm wide (1-in. \times 2-in.) notch removed, centered about the 1/4-point adjacent to the pin support.

For each test, the recorded data was processed using the techniques described previously (Peterson et al. 2001) for each test performed to obtain the modal parameters of the beam in its undamaged and damaged states. Due to noise in the recorded data, the higher modes of vibration could not be iden-

tified at the same frequencies from test to test, and the resulting mode shapes were erratic. Thus, the mode shapes for the first two modes of vibration were the only mode shapes used to locate the inflicted damage. Changes in the natural frequencies of vibration of the beam as the inflicted damage progressed are shown in Table 1.

Experimental mode shapes were reconstructed using Shannon's sampling theorem to interpolate mode shape vectors having a length of 200 points. This was done so that there were 200 points along the span where damage could possibly be located, rather than the limited number of sampling locations. Experimental mode shapes for the undamaged case and three of the damaged cases are shown in Figs. 3 and 4.

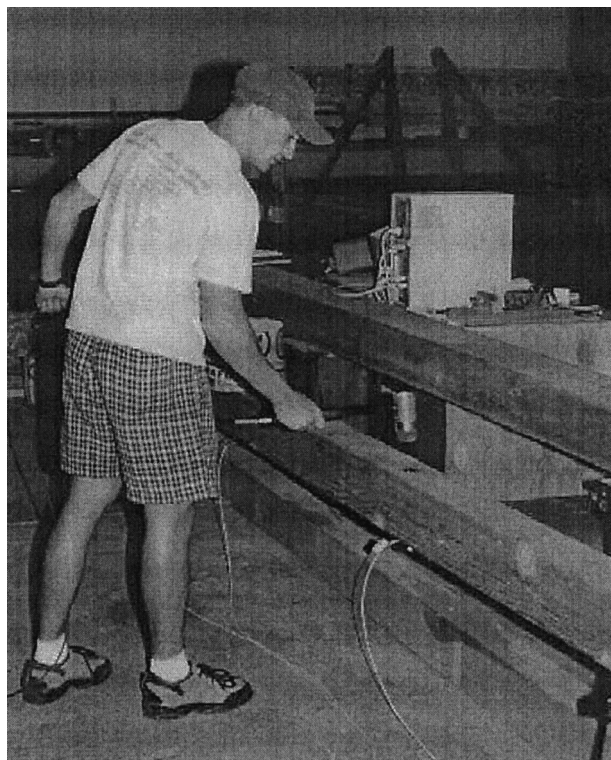


FIG. 1. Experimental Modal Testing

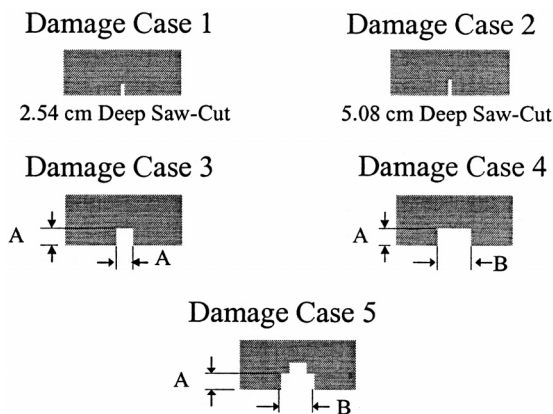


FIG. 2. Inflicted Damage on Timber Beam (A = 5.08 cm, B = 10.16 cm)

TABLE 1. Shifts in Natural Frequencies of Vibration of Experimental Beam

Damaged case (1)	Mode 1 (Hz) (2)	Mode 2 (Hz) (3)
Undamaged	11.75	55.75
1	11.75	54.75
2	11.75	51.75
3	11.25	51.75
4	10.75	50.75
5	10.50	46.25

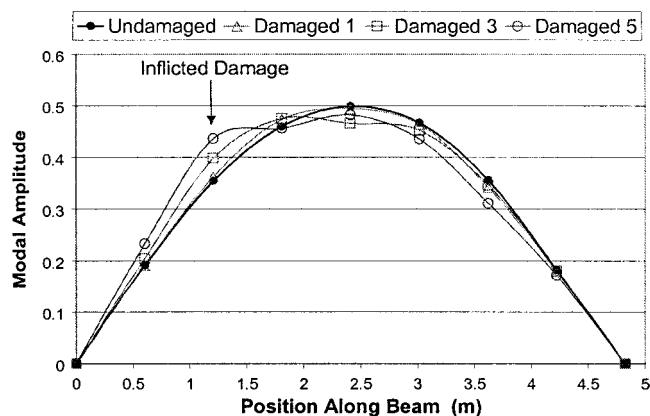


FIG. 3. Experimental Mode Shapes (Mode 1)

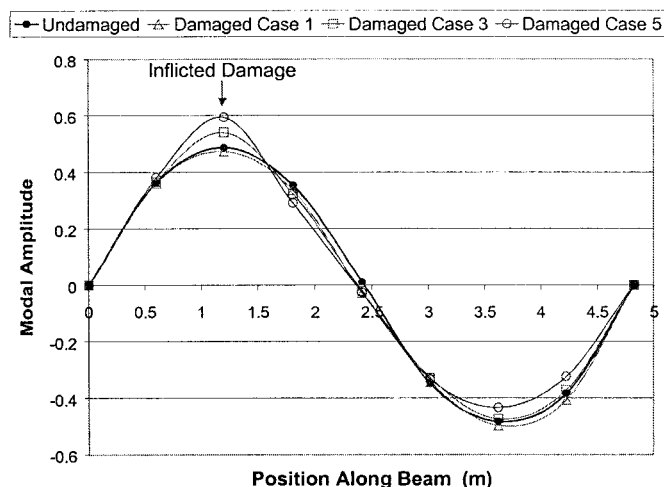


FIG. 4. Experimental Mode Shapes (Mode 2)

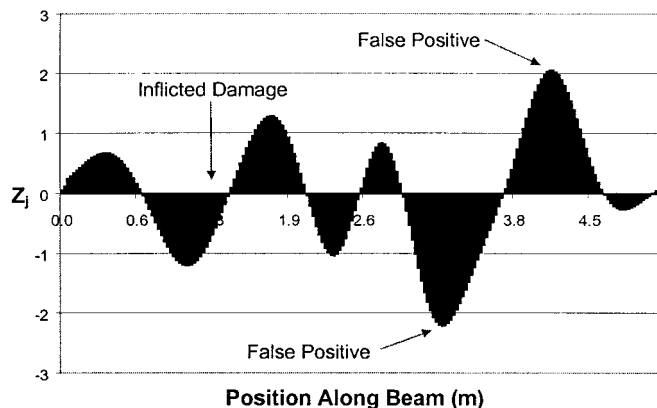


FIG. 5. Damage Indicator Values for Damage Case 1—Experimental Tests

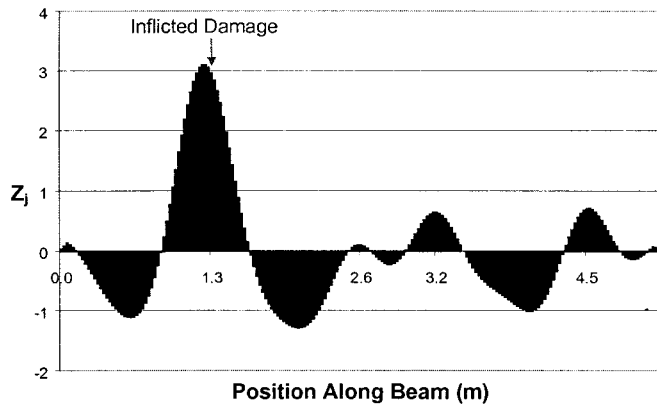


FIG. 6. Damage Indicator Values for Damage Case 2—Experimental Tests

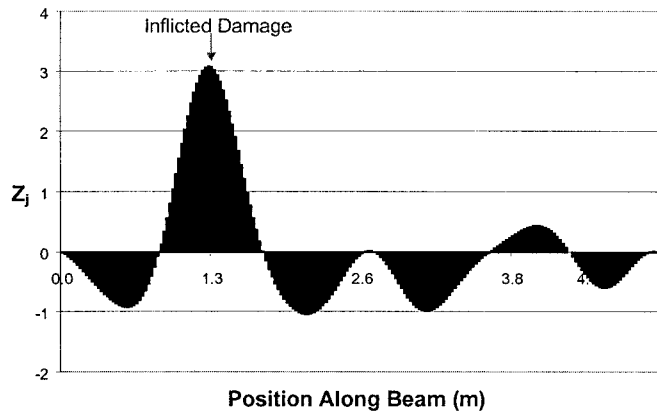


FIG. 7. Damage Indicator Values for Damage Case 3—Experimental Tests

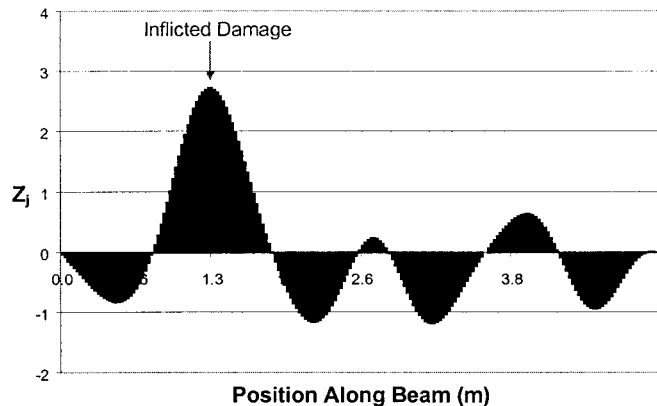


FIG. 8. Damage Indicator Values for Damage Case 4—Experimental Tests

Reconstructed experimental mode shapes were then used in the damage indicator algorithm to attempt to locate the inflicted damage. Bar graphs of the standard normal damage indicator values (Z_j) for each damage case are shown in Figs. 5–9. The damage indicator (DI) values in each figure were obtained by combining the DI values for the first and second modes of vibration [see (10) in Peterson et al. (2001)].

If the confidence interval is set such that $Z_j > 2$ (approximately 95% confidence) indicates damage at member j , the following observations can be made. For damage case 1, the damage indicator algorithm is unable to locate the 2.54-cm (1-in.) deep saw cut, and the algorithm also identifies two false locations of damage. Beginning with damage case 2, the damage indicator algorithm correctly locates the inflicted damage, with no false-positive locations of damage elsewhere along the

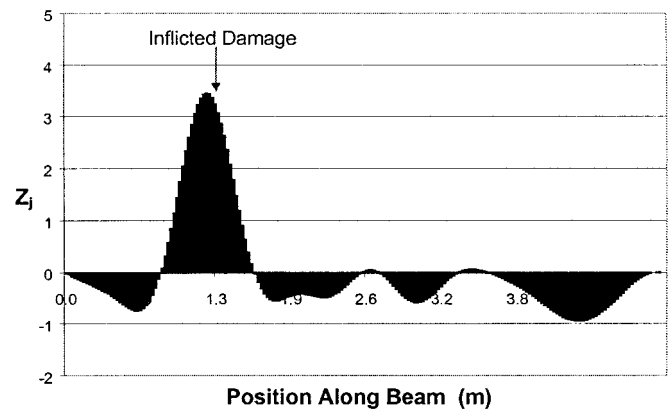


FIG. 9. Damage Indicator Values for Damage Case 5—Experimental Tests

span of the beam. For damage cases 3 and 4, the damage indicator values near the location of inflicted damage do not increase in magnitude, but the width of the spike does show an increase. A magnitude increase from that of damage case 2 for the spike in the damage indicator plot is not expected since the depth of inflicted damage was not increased for damage cases 3 and 4. For damage case 5, Fig. 9 shows an increase in the magnitude of the spike near the location of simulated damage. This is expected since the depth of the inflicted damage is increased for damage case 5. In summary, the testing of a single, simply supported timber beam in the laboratory shows that the damage indicator developed previously (Stubbs et al. 1995) is effective in locating damage in the timber beam.

USE OF CALIBRATED BASELINE MODEL FOR LOCATION OF DAMAGE

To test the use of the baseline model to locate damage in a timber structure, a baseline model of the 11.43 cm \times 15.88 cm (4.5 in. \times 6.25 in.) timber beam previously tested in the laboratory was constructed. The initial model was constructed using the Euler-Bernoulli beam element stiffness matrix with the added consideration of shear deformation. A lumped mass matrix was used to represent the mass distribution of the beam. The model consisted of 60 beam elements with both vertical and rotational degrees of freedom at each node, supported on vertical axial springs at each end. Before solving the eigenproblem, the rotational degrees of freedom were condensed out of the stiffness matrix using static condensation. The lumped mass matrix did not consider rotational inertia at the element nodes.

The best results in the calibration process of the beam were obtained by adjusting the modulus of elasticity and the modulus of rigidity of the beam elements as well as adjusting the stiffness of the supports. Note that the modulus of elasticity for an element can be changed independently from the modulus of rigidity (and vice versa), but each of the beam elements in the structure must have the same element stiffness matrix. An attempt was made to modify the stiffness of each element of the beam to account for the variation in the material properties along the span. This resulted in a model that was severely underdetermined and convergence could not be achieved due to the limited number of frequencies of vibration that could be experimentally measured. Furthermore, it is doubtful that the recorded vibration data contains enough information to accurately assess the differences in material properties along the length of the timber beam. Therefore, it was concluded that the material property values for all j elements must be consistent throughout the model.

The model was calibrated as discussed previously (Peterson et al. 2001). Stiffness properties of the calibrated beam model

are as follows: $E_x = 19.3 \text{ GPa}$ ($2.8 \times 10^6 \text{ psi}$) and $G_{xy} = 0.5 \text{ GPa}$ ($7.3 \times 10^4 \text{ psi}$) ($\sim 2.5\%$ of E_x). Based on average material property values for a Douglas fir beam, it is noted that the calibration process yields a reasonable model when convergence is reached. The first two modes of vibration were used to calculate DI values at 200 points along the span of the beam model. Standard normal DI values (Z_j) are shown in Figs. 10–14 for each of the five previously discussed experimental damage cases using the mode shapes obtained from the calibrated beam model to represent the undamaged state.

The confidence interval was set such that $Z_j > 2$ (approximately 95% confidence) indicates damage at member j and the following observations were made. For damage cases 3–5, the inflicted damage could be located without false-positive indi-

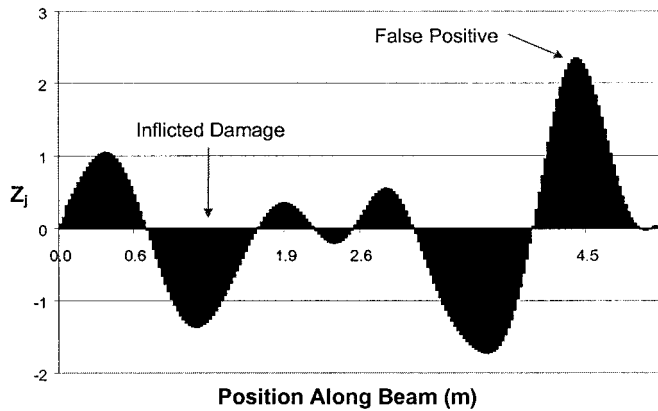


FIG. 10. Damage Indicator Values for Damage Case 1—Calibrated Beam Model

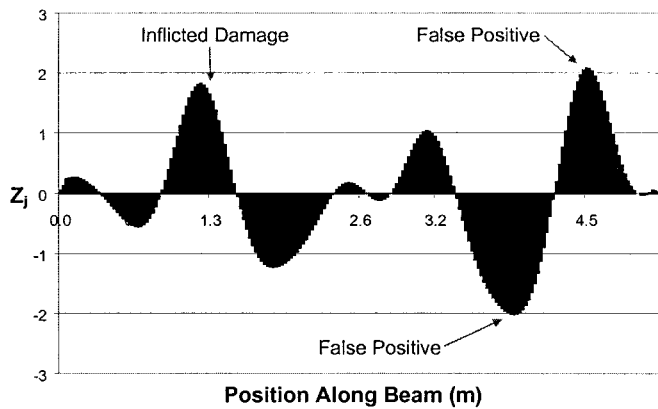


FIG. 11. Damage Indicator Values for Damage Case 2—Calibrated Beam Model

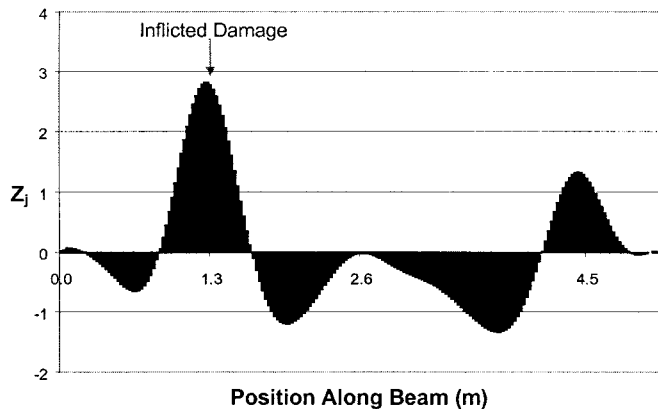


FIG. 12. Damage Indicator Values for Damage Case 3—Calibrated Beam Model

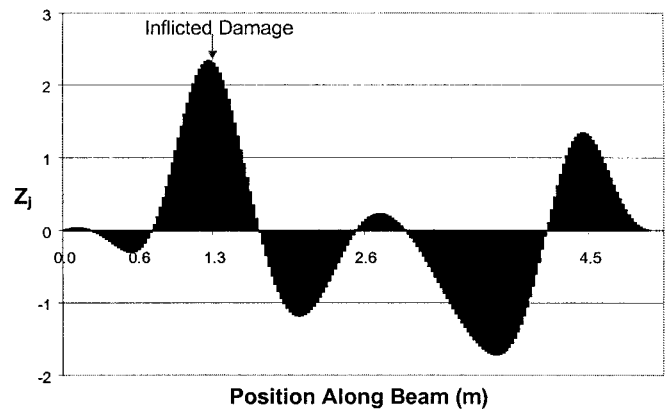


FIG. 13. Damage Indicator Values for Damage Case 4—Calibrated Beam Model

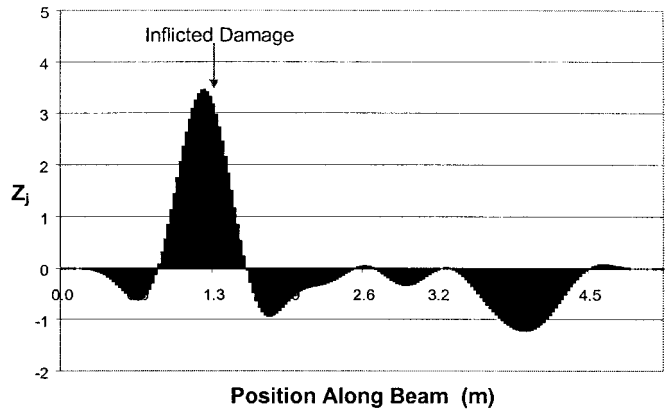


FIG. 14. Damage Indicator Values for Damage Case 5—Calibrated Beam Model

cations of damage. The magnitude Z_j at the location of inflicted damage for damage cases 3–5 is slightly less than that of the corresponding Z_j value for the damage indicator plots using the experimentally measured modal parameters for the undamaged beam (Figs. 5–9). Similar trends in the damage detection can be seen in plots for damage cases 3–5 as were noted in the plots using the experimentally obtained undamaged mode shapes (cf. Figs. 10–14 with Figs. 5–9).

For damage cases 1 and 2, inflicted damage could not be located using the baseline model to represent the undamaged state of the beam. If the confidence interval is selected such that $Z_j > 1.5$ (approximately 87% confidence) indicates damage at member j , the inflicted damage could be located for damage case 2, with two false-positive indications of damage in the beam.

It should be noted that the calibrated beam model represents an approximation of the undamaged state of the beam or structure. Thus, a greater magnitude of inflicted damage is required before the damage can be located as compared to the case where the undamaged modal parameters are available for the structure.

APPLICATION OF DYNAMIC SYSTEM IDENTIFICATION TO SEVERELY DECAYED TIMBER BEAM

To explore the use of the method developed above for global evaluation of timber members, a severely decayed timber beam was evaluated in a laboratory setting. The beam was a creosote-treated member measuring approximately $20 \text{ cm} \times 35 \text{ cm}$ (8 in. \times 13.75 in.) in cross section and approximately 2.9 m (9.5 ft) in span (Fig. 15). It is believed that the beam was, at the time of treatment with creosote, longer than the

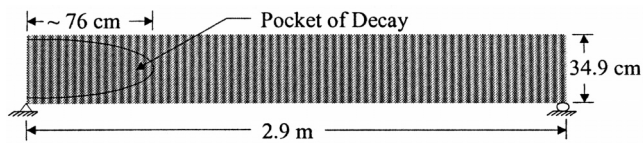


FIG. 15. Extent of Pocket of Decay within Timber Beam (Identified through Ultrasonic Tests)

span indicated above. Apparently the beam had been cut, creating an untreated end exposed to the elements for a number of years. Thus, the untreated end of the beam had experienced severe decay, while the treated, uncut end remained relatively sound.

The beam was simply supported and impact vibration tests were performed as outlined previously. The beam was impacted at the 1/4-point adjacent to the roller support (located at the sound end). The acceleration response was measured at each 1/6-point along the span along the neutral axis of the beam. The acceleration response was also measured over the supports, with the accelerometers attached near the neutral axis. The impact force and acceleration response data were sampled at 1,000 Hz with a total of 4,096 points recorded for each channel. Recorded data were transformed into the frequency domain using signal processing techniques presented previously (Peterson et al. 2001). Resulting frequency response functions from 10 individual tests were averaged to obtain the modal parameters needed (natural frequencies of vibration and mode shapes). Only the first mode of vibration could be confidently identified from the experimental data recorded, and thus the first mode was the only mode used to attempt to detect and locate the region of decay.

From the experimental tests, a significant modal amplitude was found at the sampling location over the support at the decayed end of the beam. The remaining cross section of the beam at the decayed end was essentially a thin shell approximately 1.27-cm to 2.54-cm (1/2-in. to 1-in.) thick, as seen in Fig. 16. Thus, it was concluded that the spike in the frequency response function (FRF) at the decayed end indicated compression of the end of the beam during the impact vibration tests. At the sound end of the beam, a spike in the FRF was also noted for the first mode of vibration during the data analysis. It was concluded that this spike also indicated some amount of compression perpendicular to the grain of the beam, although the magnitude of this spike was much smaller than the magnitude of the spike in the FRF over the decayed end support. It follows that some vibration caused by compression perpendicular to the grain would have been measured since the beam is very stiff for the span length used. Thus, the experimental mode shape seen in Fig. 17 is likely a combination of compression perpendicular to the grain of the beam with a small contribution from flexure.

A plane-stress finite-element model was constructed as a baseline model to obtain mode shapes representative of the undamaged state of the beam. The model was only roughly calibrated using the previously outlined calibration process. In the experimental testing, it was uncertain what contribution to the vibration measured at the support was due to the movement of the supports and what contribution was due to the compression of the beam near the severe pocket of decay located over the pin support. Thus, the stiffness of the end supports in the finite-element model were allowed to remain rigid. This is justified in that the supports were much stiffer than the beam (perpendicular to the grain), with the decayed pocket causing the one end to be even more flexible. Thus, analytical mode shapes with zero displacement at the ends (at the support point) were produced. It should be noted that the modal amplitudes shown in Fig. 17 for the finite-element model were sampled from the neutral axis of the member to be consistent



FIG. 16. Pocket of Decay

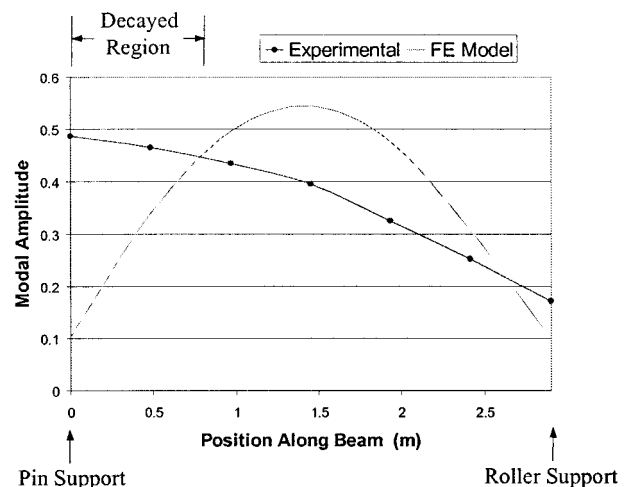


FIG. 17. Mode Shapes Used in Damage Localization Algorithm

with the sampling locations in the experimental tests. Thus, nonzero modal displacements are reflected at the ends, reflecting compression perpendicular to the grain. To further justify the rough calibration of the model, it is believed that the severe amount of decay at the end of the beam may have shifted the frequencies of vibration by a sufficient amount such that the measured frequencies of vibration may no longer accurately represent the response of the beam in its undamaged state.

In Table 2, the frequency of vibration for the first mode measured in the laboratory is compared with the first natural frequency of vibration calculated from the finite-element model. A schematic of the beam is shown in Fig. 15, indicating the extent of the pocket of decay, the location of supports, etc. A photograph showing the severe pocket of decay at the pin-supported end of the beam is shown in Fig. 16. Mode shapes used in calculating the damage indicator values are also shown

TABLE 2. Comparison of Natural Frequencies of Vibration (Baseline Model versus Experimental)

(Hz) (1)	Experimental (2)	FEM (3)	Percent difference (4)
f_1	34.2	31.9	6.7

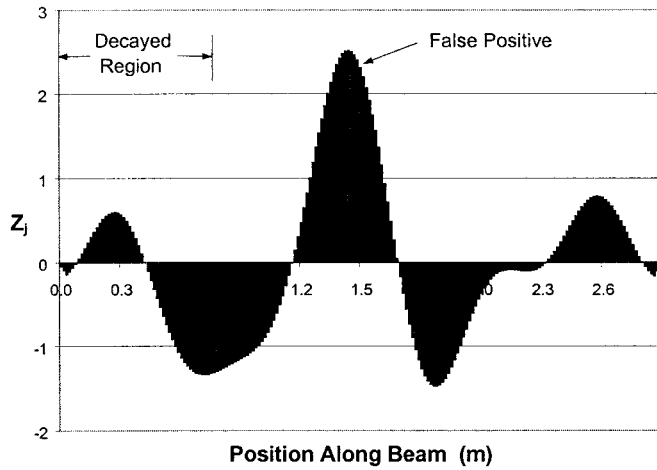


FIG. 18. Damage Indicator Values for Severely Decayed Timber Beam (Mode Considered: 1)

in Fig. 16, and the standard normal damage indicator values (Z_j) are shown in Fig. 18.

If the confidence interval for indicating decay in the timber beam is set at $Z_j > 2$, the algorithm gives no indication of the pocket of decay at the end of the beam and also shows one false-positive location of damage near the midspan. However, the mode shapes themselves do indicate that some type of damage or decay is likely present at the left end, softening the end of the beam and producing the modal displacement measured at the decayed end. Since the damage localization algorithm was derived for flexural modal strain energy, the algorithm will not correctly identify damage when significant flexural modal displacements cannot be excited and measured. In this case, the beam span was very short relative to the size of the cross section. Consequently, very little flexural vibration was excited during laboratory testing. The experimental mode shape shown in Fig. 17 reflects a mode that indicates compression perpendicular to the grain of the beam rather than flexural vibration. The above laboratory test case shows that the current damage localization algorithm is limited to applications where significant flexural vibration can be excited and measured. For very short and stiff timber beams, it would likely be necessary to derive a separate algorithm based on modes of vibration that correspond to compression perpendicular to the grain in order to correctly locate a pocket of decay at one or both ends of the beam.

CONCLUSIONS

Both analytical and laboratory tests were performed on simply supported timber beams in an effort to verify the use of experimental modal analysis and a previously developed damage localization algorithm for use in detecting and locating damage in timber beams. A calibrated baseline model was also used to represent an undamaged timber beam tested in the laboratory to more closely simulate the use of the proposed NDE method when the modal parameters for the undamaged state of the beam are unavailable.

Application of the damage localization algorithm to identify the location of the inflicted damage in a simply supported

11.43 cm \times 15.88 cm (4.5 in. \times 6.25 in.) timber beam tested in the laboratory shows that the required severity of damage is between a 2.54-cm (1-in.) and 5.08-cm (2-in.) deep saw cut before the algorithm can correctly identify the location of the damage. Damage severity on this order is necessary due to the natural variability of the material properties of wood as well as the inherent noise in the experimental measurements. It is noted that the variation of the material properties along the length of the beam (especially at the locations of large knots) would appear as damage when using the damage localization algorithm, even if noise-free experimental data could be obtained. As the severity of the inflicted damage increases, the confidence in locating the damage at the correct location also increases. Furthermore, as the removed notch becomes longer, the number of locations identified as damaged also increases, reflecting the increased length of inflicted damage.

When a calibrated baseline model is used to approximate the undamaged modal parameters of the beam, the required severity of damage is increased to between a 5.08-cm (2-in.) deep saw cut and a 5.08 cm \times 5.08 cm (2 in. \times 2 in.) notch before the damage localization algorithm can correctly identify the location of the inflicted damage. Results using the calibrated baseline model to represent the undamaged state of the beam may be improved if more of the natural frequencies of vibration can be confidently measured in the laboratory. The localization algorithm may not require knowledge of higher modes to correctly locate the inflicted damage, but this will allow the model to be calibrated more precisely so that the dynamic response of the beam can be described more accurately. This issue is likely to become more important when extending the proposed method of global NDE to actual timber structures.

Due to the derivation of the damage localization algorithm, using flexural mode shapes to indicate the location of damage within a flexural member, the algorithm is limited to applications where significant flexural vibration can be excited and measured. For cases such as the decayed timber beam with a short span and relatively large cross section, the algorithm may not correctly locate present damage no matter how large the damaged or decayed region happens to be.

The use of experimental modal analysis and the damage localization method to locate damage within a timber beam or structure is believed to be practical. The outlined method of testing provides a method to perform a global evaluation of a timber member thereby locating possible areas of damage or decay within that member. Given the limitations in the minimum severity of damage that can be located in a timber beam, other NDE methods already established should be employed to perform a more comprehensive evaluation in the localized regions identified through vibration testing. This would be done to confirm that damage or decay does exist at the locations identified by the damage localization algorithm as well as to provide a better estimate of the severity of that damage or decay.

It is noted that for some of the experimental cases of damage studied, the confidence level may be set lower so that the smaller magnitudes of inflicted damage can be identified. This would also result in several false-positive locations of damage. However, in the extension of the application of the proposed method of NDE to actual timber structures, it is desirable to identify possible areas within the structure that may be locations of damage or decay, reducing the number of locations that must be investigated using other localized forms of NDE. These identified areas would then be investigated further using one or more of the localized methods to better assess the condition of the member at the potential damage location and provide a more comprehensive evaluation of the structure. A limited number of false-positive locations of damage to be investigated further would be considered acceptable.

Each of the laboratory tests performed were simply supported beam cases. While the damage could be located within a simple beam, timber structures such as bridges are more complex, and therefore further laboratory tests should be performed to explore the capabilities and limitations of applying dynamic system identification for use in identifying damage or decay within a more complex structure.

ACKNOWLEDGMENTS

Funding for this project was provided by the U.S. Federal Highway Administration and the USDA Forest Service Forest Products Laboratory. The writers wish to thank Dr. Robert Ross at the Forest Products Laboratory for his assistance on the project as well as Dr. Sooyong Park at Texas A&M University for his suggestions concerning the implementation of the damage localization algorithm for use in timber beams.

APPENDIX I. REFERENCES

- Bolton, R., Stubbs, N., Park, S., and Choi, H. (1998). "Analysis of Lavic Road overcrossing field data." *Engrg. Technol. Dept.*, Texas A&M University, College Station, Tex.
- Emerson, R. N., Pollock, D. G., Kainz, J. A., Fridley, K. J., McLean, D. I., and Ross, R. J. (1998). "Nondestructive evaluation techniques for timber bridges." *Proc., 1998 World Conf. on Timber Engrg. (WCTE)*, Presses Polytechniques et Universitaires Romandes, 670–677.

- Peterson, S. T., et al. (2001). "Application of dynamic system identification to timber beams. I." *J. Struct. Engrg.*, ASCE, 127(4), 418–425.
- Stubbs, N., and Garcia, G. (1996). "Application of pattern recognition to damage localization." *Microcomputers in Civ. Engrg.*, 11, 395–409.
- Stubbs, N., Kim, J. T., and Farrar, C. R. (1995). "Field verification of a nondestructive damage localization and severity estimation algorithm." *Proc., 13th Int. Modal Anal. Conf.*, 210–218.
- Stubbs, N., Park, S., and Sikorski, C. (1997). "A general methodology to nondestructively evaluate bridge structural safety." *Tech. Rep. No. NDD 04-97-04 Submitted to State of California, Department of Transportation, Sacramento, Calif.*, Texas Engrg. Experimental Station, Texas A&M University, College Station, Tex.
- Stubbs, N., Sikorski, C., Park, S., Choi, S., and Bolton, R. (1998). "A methodology to nondestructively evaluate the structural properties of bridges." *Proc., 5th CALTRANS Seismic Res. Workshop*, California Department of Transportation Service Center.

APPENDIX II. NOTATION

The following symbols are used in this paper:

- E_x = longitudinal modulus of elasticity;
 f_i = natural frequency of vibration for mode i (Hz);
 G_{xy} = modulus of rigidity; and
 Z_j = standard normal damage indicator value for element j .